J|A|C|S
ARTICLES
Published on Web 09/13/2006

Structure Determination of Protein−Ligand Complexes by Transferred Paramagnetic Shifts

Michael John,[†] Guido Pintacuda,[‡] Ah Young Park,[†] Nicholas E. Dixon,[†] and Gottfried Otting*,[†]

Contribution from the Australian National University, Research School of Chemistry, Canberra, ACT 0200, Australia, and Ecole Normale Superieure de Lyon, Laboratoire de Chimie, 46 Allee d'Italie, 69364 Lyon, France.

Received May 30, 2006; E-mail: go@rsc.anu.edu.au

Abstract: Rational drug design depends on the knowledge of the three-dimensional (3D) structure of complexes between proteins and lead compounds of low molecular weight. A novel nuclear magnetic resonance (NMR) spectroscopy strategy based on the paramagnetic effects from lanthanide ions allows the rapid determination of the 3D structure of a small ligand molecule bound to its protein target in solution and, simultaneously, its location and orientation with respect to the protein. The method relies on the presence of a lanthanide ion in the protein target and on fast exchange between bound and free ligand. The binding affinity of the ligand and the paramagnetic effects experienced in the bound state are derived from concentration-dependent ^{1}H and ^{13}C spectra of the ligand at natural isotopic abundance. Combined with prior knowledge of the crystal or solution structure of the protein and of the magnetic susceptibility tensor of the lanthanide ion, the paramagnetic data define the location and orientation of the bound ligand molecule with respect to the protein from simple 1D NMR spectra. The method was verified with the ternary 30 kDa complex between the lanthanide-labeled N-terminal domain of the ϵ exonuclease subunit from the *Escherichia coli* DNA polymerase III, the subunit θ, and thymidine. The binding mode of thymidine was found to be very similar to that of thymidine monophosphate present in the crystal structure.

Introduction

In many cases, the three-dimensional (3D) structures of complexes between protein targets and low-molecular weight lead compounds can be determined from cocrystals by X-ray crystallography.[1] If crystallization is not possible, NMR spectroscopy can be used to obtain this information in solution, although the high molecular weight of many drug targets and the concomitant spectral overlap often hinder effective analysis by NMR. Here we present a novel, highly efficient NMR method for determination of the binding mode of a low molecular weight ligand molecule on the target protein. The method relies on the paramagnetism of a lanthanide ion bound to the target protein near the ligand binding site and rapid exchange between bound and free ligand. In addition to identification of the binding site, the method provides the 3D conformation of the bound ligand and its orientation and location with respect to the magnetic susceptibility anisotropy tensor $\Delta\chi$ of the lanthanide ion. If the $\Delta\chi$ tensor can be anchored in the protein structure—which is readily achieved with ^{15}N-labeled samples and prior knowledge of the protein structure from X-ray crystallography or NMR—[2,3]this results in a 3D model of the entire protein−ligand complex.

It is well recognized that pseudocontanct shifts (PCS) induced by paramagnetic metal ions can provide a source of valuable structural restraints for the determination of the 3D structures of metalloproteins[4,5] or their stoichiometric complexes with other proteins[6,7] or DNA.[8] PCS are manifested in the NMR spectrum as large changes in chemical shifts. They depend on the position of the nuclear spin with respect to the magnetic susceptibility anisotropy ($\Delta\chi$) tensor of the metal ion as[9]

$$\Delta\delta^{\mathrm{PCS}} = \frac{1}{12\pi r^3}\left[\Delta\chi_{\mathrm{ax}}(3\cos^2\theta - 1) + \frac{3}{2}\Delta\chi_{\mathrm{rh}}\sin^2\theta\cos 2\varphi\right] \quad (1)$$

where $\Delta\delta^{\mathrm{PCS}}$ denotes the difference in chemical shifts measured between diamagnetic and paramagnetic samples, $\Delta\chi_{\mathrm{ax}}$ and $\Delta\chi_{\mathrm{rh}}$ are the axial and rhombic components of the $\Delta\chi$ tensor, and r, θ, and φ are the spherical coordinates of the nuclear spin in the principal axis frame of the $\Delta\chi$ tensor. Three additional angles, e.g., the Euler angles α, β, and γ, describe the orientation of the principal axis frame with respect to the molecule or complex.

[†] Australian National University.
[‡] Ecole Normale Superieure de Lyon.

(1) Davis, A. M.; Teague, S. J.; Kleywegt, G. J. *Angew. Chem., Int. Ed.* **2003**, *42*, 2718−2736.
(2) Pintacuda, G.; Keniry, M. A.; Huber, T.; Park, A. Y.; Dixon; N. E.; Otting, G. *J. Am. Chem. Soc.* **2004**, *126*, 2963−2970.
(3) Schmitz, C.; John, M.; Park, A. Y.; Pintacuda, G.; Dixon, N. E.; Otting, G.; Huber, T. *J. Biomol. NMR* **2006**, *35*, 79−87.
(4) Banci, L.; Bertini, I.; Cremonini, M. A.; Gori-Savellini, G.; Luchinat, C.; Wüthrich, K.; Güntert, P. *J. Biomol. NMR* **1998**, *12*, 553−557.
(5) Allegrozzi, M.; Bertini, I.; Janik, M. B. L.; Lee, Y.-M.; Liu, G.; Luchinat, C. *J. Am. Chem. Soc.* **2000**, *122*, 4154−4161.
(6) Ubbink, M.; Ejdebäck, M.; Karlsson, B. G.; Bendall, D. S. *Structure* **1998**, *6*, 323−335.
(7) Díaz-Moreno, I.; Díaz-Quintana, A.; De la Rosa, M. A.; Ubbink, M. *J. Biol. Chem.* **2005**, *280*, 18908−18915.
(8) Tu, K.; Gochin, M. *J. Am. Chem. Soc.* **1999**, *121*, 9276−9285.
(9) Bertini, I.; Luchinat, C.; Parigi, G. *Prog. Nucl. Magn. Reson. Spectrosc.* **2002**, *40*, 249−273.

10.1021/ja063584z CCC: $33.50

In the following we report the structure of the 30 kDa complex between a lanthanide (Ln^{3+})-labeled protein, the N-terminal domain of the subunit ϵ bound to the subunit θ of the *Escherichia coli* DNA polymerase III ($\epsilon 186/\theta$), and a small ligand molecule, thymidine. Similar to the related domain of DNA polymerase I,[10] $\epsilon 186$ has a high affinity ($K_D < 10\ \mu M$) for single lanthanide ions in the active site, and stoichiometric complexes $\epsilon 186/\theta/Ln^{3+}$ are easily obtained by the addition of equimolar amounts of $LnCl_3$. For $Ln^{3+} = Dy^{3+}$, Tb^{3+}, and Er^{3+} we have recently determined reliable $\Delta\chi$-tensor parameters including the position of the metal ion, using amide PCS of $\epsilon 186$ from ^{15}N-HSQC and HNCO spectra.[3] These tensor parameters predict not only large pseudocontact shifts for the entire active site but also line broadening beyond detection for all ^{1}H spins within about 15 Å.

Thymidine rapidly exchanges between the free state and the $\epsilon 186/\theta/Ln^{3+}$/thymidine complex so that the information about the PCS in the bound state is transferred to the averaged NMR signal. With a large excess of thymidine, "transferred PCS" could thus be measured with NMR spectra closely resembling those of free thymidine, including reasonably narrow linewidths. Transferred PCS and transferred paramagnetic line broadenings were used to measure binding affinities, and the structure of the protein−ligand complex was derived using transferred PCS observed in the ^{1}H and ^{13}C NMR spectra of thymidine. The binding mode of thymidine is shown to be closely similar to that of thymidine monophosphate (TMP) in the cocrystal with $\epsilon 186$.[11]

Materials and Methods

Sample Preparation. All experiments were carried out on 120 μM samples of the protein complex $\epsilon 186/\theta$ with ^{15}N-labeled $\epsilon 186$ and unlabeled θ, which was prepared as described previously.[12] The NMR buffer contained 20 mM Tris (tris(hydroxymethyl) methylamine) at pH 7.2, 100 mM NaCl, 0.1 mM dithiothreitol, and 0.01% (w/v) NaN_3, with 90% H_2O and 10% D_2O. The 1:1 complexes of $\epsilon 186/\theta$ with Ln^{3+} ions (Ln = La, Dy, Tb, Er) were prepared by addition of 12 μL of buffered $LnCl_3$ solution (5 mM) to 500 μL of the protein complex and inspected by ^{15}N-HSQC spectra. Thymidine was added as a 200 mM buffered solution in volumes of $V = 2.5$, 5, 25, 45, 85 and 165 μL, resulting in ligand/protein ratios of about 8, 16, 80, 150, 280, and 550, respectively. Ligand and protein concentrations at each titration step were calculated according to $c_L = 200\ mM \times V/(512\ \mu L + V)$ and $c_P = 120\ \mu M \times 500\ \mu L/(512\ \mu L + V)$.

NMR Spectroscopy. All NMR spectra were acquired at 25 °C and a ^{1}H NMR frequency of 800 MHz on a Bruker AV800 NMR spectrometer equipped with a triple-resonance (TCI) cryogenic probe. ^{15}N-HSQC spectra were recorded with 16 transients and 64 complex t_1 increments in typically 40 min. ^{1}H NMR spectra were recorded with 8 scans and a recovery delay of 3 s, using Watergate[13] for water suppression. No substantial shifts of the water and buffer resonances were observed in the presence of 120 μM lanthanides or 50 mM thymidine. ^{13}C NMR spectra of the different samples were recorded at the final ligand/protein ratio of 550, using proton decoupling during acquisition and 1024 scans with a recovery delay of 1 s. The individual resonances were fitted to a Lorentzian line shape using Mathematica (Wolfram Research, Champaign, IL). Experimental frequency uncertainties were estimated as ±10% of the sum of linewidths (full width at half-height) of paramagnetic and diamagnetic peaks.

Structure Calculations. The Xplor[14,15] calculations consisted of conventional Powell minimizations in Cartesian coordinate space, with a target function including a purely repulsive van der Waals potential, the measured PCS values as the only experimental restraints, and a term for idealized covalent geometry as provided by the Charmm19 empirical energy function. The protocol was modified from a protocol designed for RDC-driven docking[16] and employed the previously reported $\Delta\chi$-tensor parameters.[3] The protein backbone atoms and the pseudoresidues defining the metal coordinates and the principal axis system of the $\Delta\chi$ tensor were held fixed with respect to the coordinates of $\epsilon 186$ (PDB entry 1J53).[11] Thymidine was modeled after the TMP molecule 2000 of the crystal structure and translated 50 Å away from $\epsilon 186$. An initial phase (1000 steps) of unrestrained high-temperature (3000 K) dynamics was used to randomize the starting geometries. The docking procedure involved 110 cycles (500 steps per cycle) in which the force constants for the pseudocontact (kpcs) and repulsive van der Waals (kvdw) terms were ramped from 0.1 to 1 kcal mol^{-1} ppm^{-2}, and from 0.001 to 1.0 kcal mol^{-1} Å^{-4}, respectively, with the van der Waals radii scaled (svdw) to 0.8 times their values in the Charmm19 parameters. The resulting structures were minimized using 1000 steps of dynamics with the force constants unchanged.

Results

Binding of TMP and Thymidine. The crystal structure of $\epsilon 186$ features two Mn^{2+} ions in the active site which are coordinated by the phosphate group of a TMP molecule.[11] We found that, in the presence of di- or trivalent metal ions, titration of $\epsilon 186/\theta$ with TMP in solution gives rise to ^{15}N-HSQC perturbations which are in agreement with this TMP binding site. Furthermore, increasing TMP concentrations result in a strong shift of the relatively well resolved and narrow Met18-$C^{\epsilon}H_3$ signal of $\epsilon 186$ in the 1D ^{1}H NMR spectrum. This methyl group directly contacts the thymine moiety of TMP in the crystal structure. TMP binding strongly depends on the presence of metal ions in the active site of $\epsilon 186/\theta$ (see Table S1 in the Supporting Information), thereby confirming a direct TMP−metal interaction in solution. Since such a contact in the $\epsilon 186/\theta/Ln^{3+}$ complex is likely to affect the $\Delta\chi$ tensor of the lanthanide ion, we subsequently used the electrostatically neutral nucleoside thymidine instead of TMP. On the basis of chemical shift changes observed in ^{15}N-HSQC spectra, it is seen that thymidine and TMP bind to the same site with similar affinities (K_D = 7.6 mM and 8.6 mM) in the presence of La^{3+}. In contrast to TMP, the measured affinities of thymidine to $\epsilon 186/\theta$ are largely independent of the absence and presence of metal ions. ^{15}N-HSQC spectra of the $\epsilon 186/\theta/Ln^{3+}$ complexes, recorded in the absence and the presence of 50 mM thymidine (corresponding to about 90% saturation), also confirmed that the $\Delta\chi$ tensor is not affected by ligand binding.

Paramagnetic Effects in ^{1}H NMR Spectrum of Thymidine. Figure 1A shows the ^{1}H NMR resonance of the methyl group of thymidine at various concentrations of thymidine in the presence of $\epsilon 186/\theta$ loaded with Er^{3+}. The thymidine methyl peak of a diamagnetic sample, where $\epsilon 186/\theta$ was loaded with La^{3+}, is also shown as a reference. Whereas at concentrations

(10) Frey, M. W.; Frey, S. T.; Horrocks, W. D., Jr.; Kaboord, B. F.; Benkovic, S. J. *Chem. Biol.* **1996**, *3*, 393−403.
(11) Hamdan, S.; Carr, P. D.; Brown, S. E.; Ollis, D. L.; Dixon, N. E. *Structure* **2002**, *10*, 535−546.
(12) Hamdan, S.; Bulloch, E. M.; Thompson, P. R.; Beck, J. L.; Yang, J. Y.; Crowther, J. A.; Lilley, P. E.; Carr, P. D.; Ollis, D. L.; Brown, S. E.; Dixon, N. E. *Biochemistry* **2002**, *41*, 5266−5275.
(13) Piotto, M.; Saudek, V.; Sklenar, V. *J. Biomol. NMR* **1992**, *2*, 661−665.
(14) Schwieters, C. D.; Kuszewski, J. J.; Tjandra, N.; Clore, G. M. *J. Magn. Reson.* **2003**, *160*, 66−74.
(15) Banci, L.; Bertini, I.; Cavallaro, G.; Giachetti, A.; Luchinat, C.; Parigi, G. *J. Biomol. NMR* **2004**, *28*, 249−261.
(16) Clore, G. M. *Proc. Natl. Acad. Sci. U.S.A.* **2000**, *97*, 9021−9025.

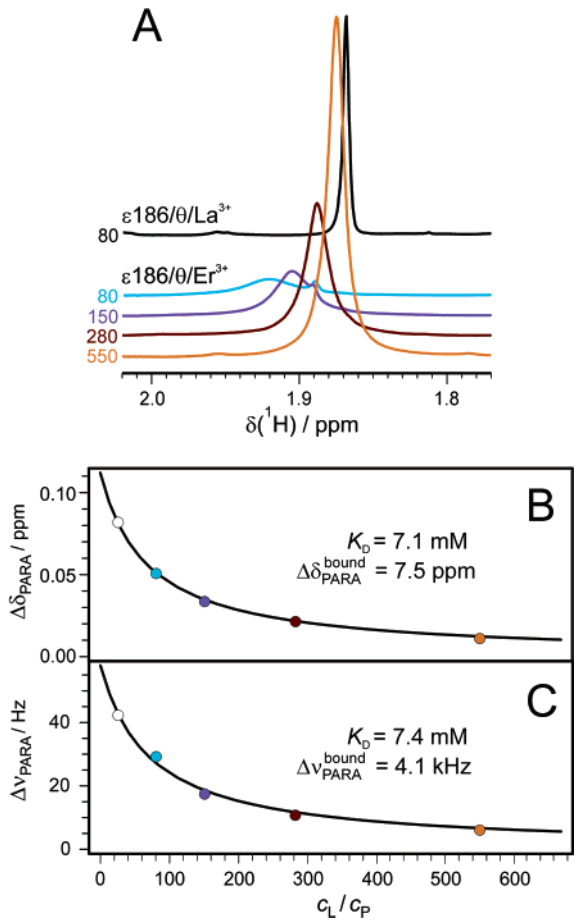

Figure 1. (A) ^{1}H NMR resonance of the methyl group of thymidine in the presence of diamagnetic ϵ186/θ/La^{3+} and paramagnetic ϵ186/θ/Er^{3+} at increasing thymidine concentrations. The spectra are labeled with the ligand/protein ratio. The weak peak at 1.89 ppm originates from the protein. (B) Paramagnetic shift and (C) paramagnetic line broadening (= line width at half-height minus line width observed in the diamagnetic spectrum) of the methyl ^{1}H NMR resonance plotted versus the ligand/protein ratio. The solid line represents the best fit to eqs 2 and 3.

below 2 mM, corresponding to a 16-fold ligand excess, thymidine remains completely invisible in the ^{1}H NMR spectrum of the paramagnetic sample, increasing concentrations result in narrowing of the methyl peak and a shift toward its position in the diamagnetic reference. Similar effects are observed for the other NMR signals of thymidine and in the presence of the lanthanides Tb^{3+} and Dy^{3+}.

In the case of Dy^{3+}, many of the thymidine ^{1}H resonances are so strongly paramagnetically broadened that they only become visible at a ligand concentration of 50 mM, which corresponds to a 550-fold excess over the protein (see Figure S1 in the Supporting Information). In contrast, the diamagnetic reference spectrum is largely independent of the thymidine concentration and closely resembles the spectrum of the free ligand. Likewise, little line broadening and no paramagnetic shifts are observed for thymidine if only the lanthanides Dy^{3+}, Tb^{3+}, or Er^{3+} but not ϵ186/θ are present in solution (data not shown).

Deriving the Binding Affinity of Thymidine from Paramagnetic Effects. The spectral changes observed in Figure 1A can be explained by strong paramagnetic effects experienced in the bound state which, due to fast exchange between bound and free state, are transferred to the average spectrum and scaled down by the fraction f^{bound} of bound versus free thymidine. The paramagnetic shift $\Delta\delta_{\text{PARA}}$ and line broadening $\Delta\nu_{\text{PARA}}$ are equally affected:

$$\Delta\delta_{\text{PARA}} = f^{\text{bound}}\Delta\delta_{\text{PARA}}^{\text{bound}} \text{ and } \Delta\nu_{\text{PARA}} = f^{\text{bound}}\Delta\nu_{\text{PARA}}^{\text{bound}} \quad (2)$$

Equation 2 assumes that the free ligand does not experience paramagnetic effects, and the exchange between bound and free state is sufficiently fast so that further exchange broadening can be neglected (see Supporting Information). In cases where the total ligand concentration c_L in solution is much larger than the concentration of the paramagnetic protein c_P (and therefore of the bound ligand c_L^{bound}), the fraction of the bound ligand f^{bound} can be approximated as (see Supporting Information)

$$f^{\text{bound}} = \frac{c_L^{\text{bound}}}{c_L} = \frac{c_P}{K_D + c_L} \quad (3)$$

Equation 3 readily provides access to the dissociation constant K_D using only ligand signals, as illustrated in Figure 1B,C. The K_D values derived from the paramagnetic shifts and line broadenings are very similar to that obtained from ^{15}N-HSQC (i.e., protein-) spectra of diamagnetic ϵ186/θ/La^{3+} titrated with thymidine. Knowledge of K_D then allows the calculation of f^{bound} for arbitrary protein and ligand concentrations (eq 3) and, hence, the paramagnetic shifts $\Delta\delta_{\text{PARA}}^{\text{bound}}$ and linewidths $\Delta\nu_{\text{PARA}}^{\text{bound}}$ of all thymidine signals in the bound state (eq 2).

Paramagnetic Effects in the ^{13}C NMR Spectrum. Paramagnetic line broadening $\Delta\nu_{\text{PARA}}^{\text{bound}}$ caused by lanthanide ions with fast relaxing electron spins primarily stems from dipolar relaxation with the averaged Curie spin and, for proteins with long rotational correlation time τ_R and at high magnetic field B_0, can therefore be approximated by[9]

$$\Delta\nu_{\text{PARA}}^{\text{bound}} = \frac{1}{5\pi^2 r^6}\gamma^2 B_0^2 \chi^2 \tau_R \quad (4)$$

where γ is the nuclear gyromagnetic ratio, χ is the isotropic magnetic susceptibility of the paramagnetic metal ion, and r is the distance of the nuclear spin from the paramagnetic center. The smaller gyromagnetic ratio of ^{13}C spins is thus less susceptible to paramagnetic line broadening. This can be used to extend the range of observable spins toward smaller distances r.[17]

^{13}C NMR spectra of thymidine are readily recorded at natural isotopic abundance in the samples containing 90 μM paramagnetic protein and 50 mM thymidine, corresponding to 550-fold excess or $f^{\text{bound}} = 1.6 \times 10^{-3}$. Using ^{1}H broadband decoupling, all ^{13}C resonances appear as singlets. Figure 2 compares the ^{13}C NMR spectra of thymidine in the presence of ϵ186/θ loaded with Dy^{3+} and La^{3+}, respectively. The peak intensities in the paramagnetic spectrum vary strongly due to differential broadening $\Delta\nu_{\text{PARA}}$, thus making them an excellent indicator for the relative distance of the different ^{13}C spins from the metal ion (eq 4). From Figure 2 it is immediately evident that thymidine binds with the deoxyribose moiety facing the Dy^{3+} ion, with the C4′ carbon closer to the metal ion than the C1′ carbon. Additionally, all paramagnetic ^{13}C resonances are shifted from their diamagnetic positions with their individual $\Delta\delta_{\text{PARA}}$ values.

(17) Bermel, W.; Bertini, I.; Felli, I. C.; Piccioli, M.; Pierattelli, R. *Prog. Nucl. Magn. Reson. Spectrosc.* **2006**, *48*, 25−45.

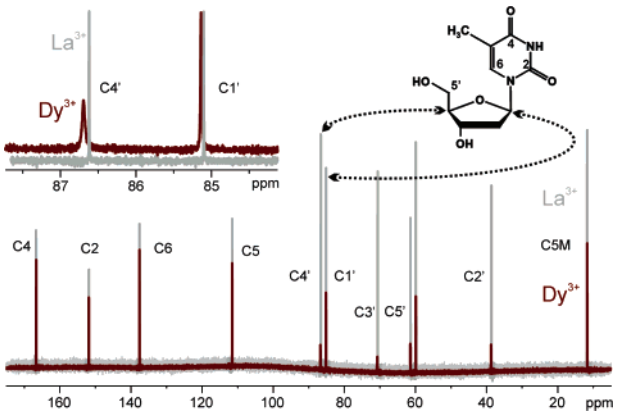

Figure 2. Natural abundance ^{13}C NMR spectra of 50 mM thymidine in the presence of 90 μM $\epsilon186/\theta/Dy^{3+}$ (red) and $\epsilon186/\theta/La^{3+}$ (gray), respectively. The diamagnetic spectrum (128 scans) is scaled 8-fold with respect to the paramagnetic spectrum (1024 scans). The signal at 60 ppm originates from Tris buffer. The resonances of C4′ and C1′ of thymidine are expanded in the insert, highlighting their different paramagnetic line broadenings and shifts.

Compared to the ^1H NMR spectrum, paramagnetic line broadening is less pronounced, and all ^{13}C resonances are well resolved, therefore allowing for precise measurement of $\Delta\delta_{PARA}$. For example, in the most broadened peak, belonging to C3′, $\Delta\nu_{PARA} = 15$ Hz is still smaller than $\Delta\delta_{PARA} = 0.113$ ppm (= 22.5 Hz).

Structure Calculation of the Complex. Using the ^1H and ^{13}C NMR spectra of thymidine recorded at 50 mM concentration ($f^{bound} = 1.6 \times 10^{-3}$), we calculated $\Delta\delta_{PARA}^{bound}$ from eq 2 for all ^1H and ^{13}C spins of thymidine in the presence of $\epsilon186/\theta/Dy^{3+}$, $\epsilon186/\theta/Tb^{3+}$, and $\epsilon186/\theta/Er^{3+}$ (see Table S2 in the Supporting Information). Diamagnetic shifts of the thymidine resonances due to binding cancel out by referencing to the diamagnetic $\epsilon186/\theta/La^{3+}$ sample containing the same concentration of thymidine. No values were obtained for H5″ as its respective resonances are very broad and partially overlapped with the buffer signal. Likewise, H2′ and H2″ yielded a single peak in all paramagnetic spectra and thus had to be given large errors of $\Delta\delta_{PARA}^{bound}$. All paramagnetic shifts were interpreted as $\Delta\delta^{PCS}$ (eq 1), as any contributions from contact shifts or residual anisotropic chemical shifts are expected to be within the error of measurement.[18] Therefore, in the following $\Delta\delta_{PARA}^{bound}$ is equated with $\Delta\delta^{PCS}$.

With the PCS data as the only experimental restraints, the structure of the $\epsilon186$/thymidine complex was calculated using Xplor-NIH,[14] modified to incorporate refinement against paramagnetic observables.[15] Four datasets were used: PCS from either $\epsilon186/\theta/Dy^{3+}$, $\epsilon186/\theta/Tb^{3+}$, and $\epsilon186/\theta/Er^{3+}$, respectively, and PCS from all three metal ions simultaneously with equal weighting. For each dataset, 20 independent calculations were performed, using the crystal structure of $\epsilon186$ (PDB entry 1J53)[11] and the previously optimized $\Delta\chi$-tensor parameters and position of the lanthanide ion.[3] This position is located approximately 0.5 Å away from the A-site Mn^{2+} ion of the crystal structure. All calculations started from random conformations, orientations, and positions of thymidine far away from the $\epsilon186$ molecule. In order to avoid trivial steric guidance of thymidine toward the "empty" TMP binding pocket of the crystal structure, all amino acid side chains were allowed to vary freely during the calculations. Finally, the 20 calculated structures were ranked by their residual PCS energy, and the best and 7 best structures were selected to represent the structure of the complex and the precision of the structure determination, respectively.

(18) John, M.; Park, A. Y.; Pintacuda, G.; Dixon, N. E.; Otting, G. *J. Am. Chem. Soc.* **2005**, *127*, 17190−17191.

Table 1. RMSD[a] (in Å) between the Seven Best Calculated Thymidine Molecules and Their Mean, and between the Calculated Thymidines and the TMP of the Crystal Structure

dataset	calculated vs mean[b]	calculated vs crystal[c]
$Dy^{3+}/Tb^{3+}/Er^{3+}$	0.08 (0.04−0.11)	0.72 (0.70−0.75)
Dy^{3+}	0.32 (0.19−0.47)	1.14 (0.96−1.40)
Tb^{3+}	0.27 (0.22−0.37)	0.78 (0.61−0.98)
Er^{3+}	0.72 (0.36−1.06)	1.20 (0.45−1.68)

[a] Using heavy atoms of thymidine/TMP following superposition of the protein backbone. Values are averaged over the seven structures, with the range given in parentheses. [b] Mean of the seven calculated structures. [c] PDB entry 1J53.[11]

Structure of the $\epsilon186$/Thymidine Complex. Independent of the dataset used to calculate the structure of the complex, thymidine was found in a location and orientation very similar to that of TMP in the crystal structure of $\epsilon186$.[11] The selected structures calculated with data from all three lanthanides yielded the smallest root-mean-square deviation (RMSD) between the thymidine coordinates and are on average closest to the crystal structure (Table 1). Figure 3A shows that these seven thymidine molecules almost completely superimpose with a RMSD between heavy atoms of only 0.08 Å. As for TMP, the deoxyribose ring is found in a 3′-endo conformation, with the thymine base oriented anti and the C4′−C5′ bond rotated such that the O5′ atom is almost eclipsed with O4′. In Figure 3B, the best structure of this family is superimposed onto the $\Delta\chi$ tensor of Er^{3+}, represented by isosurfaces of positive and negative PCS. The isosurface of zero PCS runs through the glycosidic bond of thymidine, resulting in positive $\Delta\delta^{PCS}$ for the thymine moiety and negative values for the sugar. Due to slightly different $\Delta\chi$-tensor orientations and rhombicities the zero PCS isosurfaces of the Dy^{3+} and Tb^{3+} tensors are shifted more toward the base.

The quality of the structure determination can be assessed further from the correlations between measured $\Delta\delta^{PCS}$ data and $\Delta\delta^{PCS}$ values back-calculated from the known $\Delta\chi$ tensors of Dy^{3+}, Tb^{3+}, and Er^{3+}, which are shown in Figure 4. The close agreement confirms that the observed paramagentic shifts predominantly originate from PCS. Interestingly, several directly bonded ^{13}C and ^1H spins display significantly different PCS values, i.e., the PCS helped to orient the bonds with respect to the $\Delta\chi$ tensor.[18] The agreement between measured and back-calculated $\Delta\delta^{PCS}$ improves only little for the structures calculated using a single lanthanide ion (see Figure S2 in the Supporting Information). This shows that the datasets from the three lanthanides are compatible with each other.

The improved structural definition obtained from the Dy^{3+}/Tb^{3+} versus Er^{3+} data (see Figure S3 in the Supporting Information) may be attributed to the smaller $\Delta\chi$-tensor parameters of Er^{3+}, resulting in a lesser weight of the PCS restraints compared with van der Waals restraints imposed by the protein environment. The largest deviations between measured and back-calculated $\Delta\delta^{PCS}$ are found for C5′, C4′, and C3′, and their bound protons (Figure 4), all of which are located within 6 Å distance from the metal ion. Possibly, their paramagnetic effects are modulated by residual mobility or

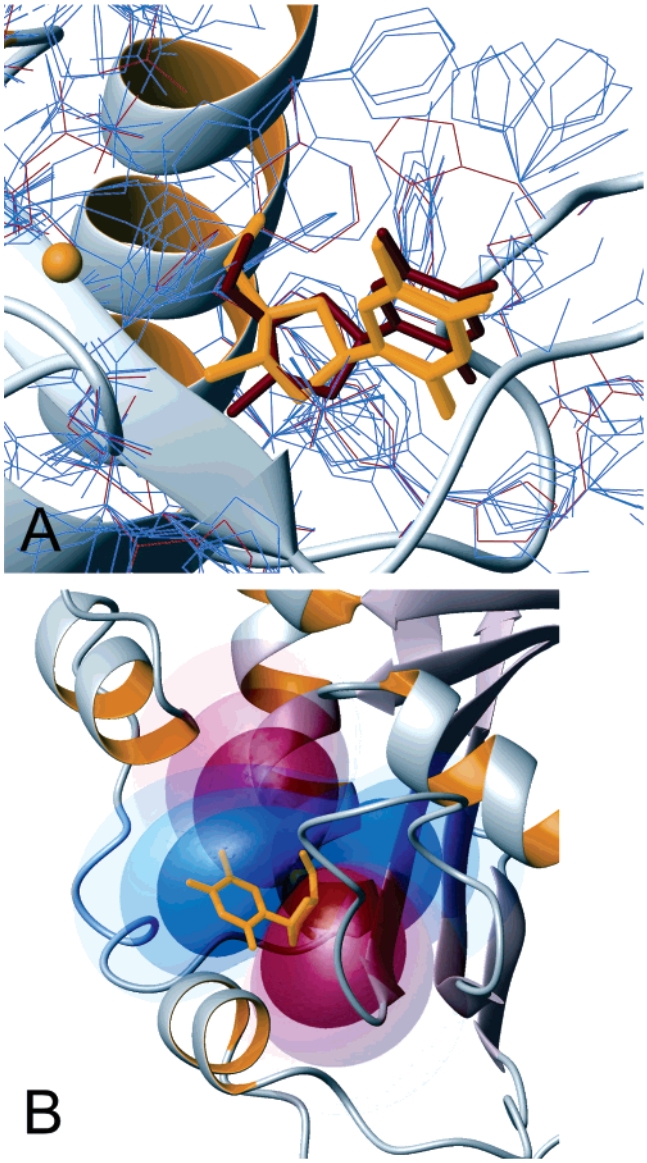

Figure 3. (A) Superposition of the seven best structures of the ϵ186/thymidine complex calculated using data from all three lanthanides Dy^{3+}, Tb^{3+}, and Er^{3+}. The protein backbone is represented as a gray and yellow ribbon. Protein sidechains and thymidine molecules from the calculated structures are shown in blue and yellow, repsectively. Protein sidechains and the TMP molecule in the crystal structure of ϵ186 are overlaid in red. (B) Best structure superimposed with the $\Delta\chi$ tensor of Er^{3+}. The tensor is represented by blue and red lobes for positive and negative PCS, respectively, contoured at PCS isosurfaces of $\pm$5, $\pm$2.5, and $\pm$1.25 ppm.

disorder in the lanthanide binding site. Notably, relatively large B-factors were reported for the bound Eu^{3+} ion in the crystal structure of the related fragment of DNA polymerase I.[19]

Discussion

Comparison with Shift Reagents. Lanthanide shift reagents have a long tradition in organic chemistry, where they are used to resolve NMR signals of compounds that are either stereochemically degenerate or otherwise overlapped.[20−22] These reagents generate PCS in the target molecule through transient complex formation, usually mediated by direct contact with the lanthanide ion. Although paramagnetic shifts have been used to derive structural restraints,[23] this application is limited by the difficulty of determining accurate $\Delta\chi$-tensor parameters: (i) The NMR signals of the shift reagent are mostly unobservable due to extreme line broadening caused by the paramagnetism. (ii) Changing the coordination of the lanthanide ion changes the $\Delta\chi$-tensor parameters. (iii) The PCS of the ligand molecule are difficult to distinguish from the contact shifts arising from direct coordination with the lanthanide ion. (iv) Any flexibility of the complex results in an averaged, effective $\Delta\chi$ tensor.

None of these issues arises in a complex between a ligand molecule and a rigid lanthanide-labeled protein. Proteins usually contain a large number of spins that are sufficiently remote from the metal center to remain observable even for the strongest paramagnetic lanthanide ions, thereby allowing the determination of accurate $\Delta\chi$ tensors. With the protein molecule mediating the lanthanide−ligand interaction, any direct lanthanide−ligand contacts and, hence, contact shifts are avoided, and the chance of modifying the $\Delta\chi$ tensor by the ligand is minimized. Any changes of the $\Delta\chi$-tensor parameters arising from ligands that directly coordinate the metal ion could be determined from ^{15}N-HSQC spectra of a ^{15}N-labeled protein sample saturated with ligand.

The protein as "shift reagent" also obliterates the need for specific functional groups on the ligand that can successfully compete with the solvent molecules for a free coordination site on the lanthanide ion. Notably, PCS observed for the ligand molecule are scaled by the ratio of complexed and free ligand f^{bound}, which depends on a principally unknown dissociation constant (eq 3). In the case of very weak binding to a conventional shift reagent, which is a situation often encountered in water or other highly polar solvents, the paramagnetic shifts on the target molecule are proportional to the reagent concentration and do not reveal the binding affinity unless very high concentrations are used. Yet, as shown here, binding with a dissociation constant in the low millimolar range is sufficient for accurate determination of K_D from the paramagnetic effects in the ligand spectrum at typical NMR concentrations. Once K_D is known, protein and ligand concentrations can be adjusted to yield the desired strength of the transferred paramagnetic effects for structural studies. For tighter binding ligands and as long as the ligand NMR signals remain observable, both protein and ligand concentrations can be substantially reduced to achieve the same f^{bound} (eq 3).

Comparison with Other Transferred NMR Effects. The observation of paramagnetic shifts and line broadening of ligand signals relies on NMR effects that are much larger in the bound state of the ligand than in its free state and on rapid exchange between the two states. Under these circumstances the bound state can be studied from the spectrum averaged with a large excess of free ligand and using protein concentrations far below the K_D value. The same principle has previously been exploited for the observation of transferred nuclear Overhauser enhancement (NOE)[24−26] and transferred cross-correlated relaxation.[27,28] However, compared with these effects, which mainly rely on

(19) Brautigam, C. A.; Aschheim, K.; Steitz, T. A. *Chem. Biol.* **1996**, *6*, 901−908.
(20) Hinckley, C. C. *J. Am. Chem. Soc.* **1969**, *91*, 5160−5162.
(21) Reuben, J. *Prog. Nucl. Magn. Reson. Spectrosc.* **1973**, *9*, 3−70.
(22) Peters, J. A.; Huskens, J.; Raber, D. J. *Prog. Nucl. Magn. Reson. Spectrosc.* **1996**, *28*, 283−350.
(23) Barry, C. D.; North, A. C. T.; Glasel, J. A.; Williams, R. J. P.; Xavier, A. V. *Nature* **1971**, *232*, 236−245.

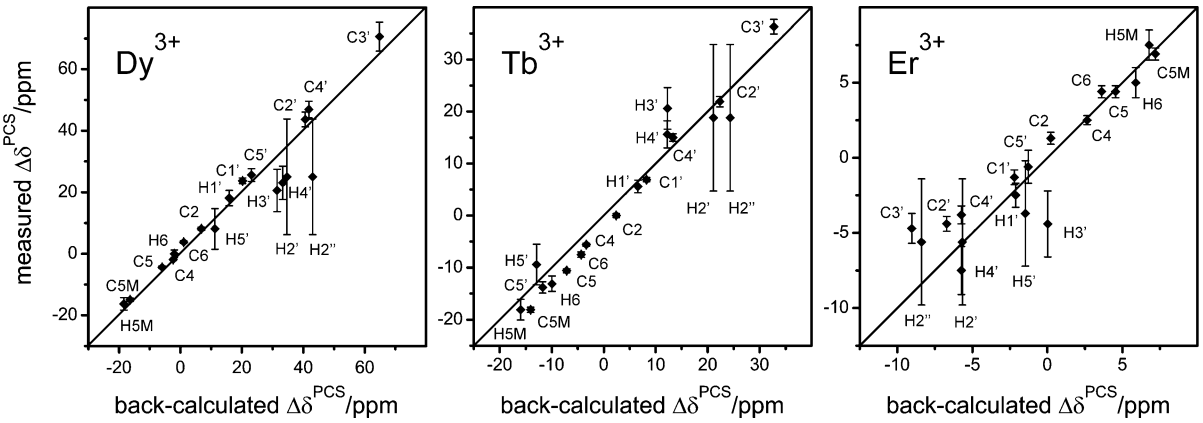

Figure 4. Correlation between measured and back-calculated ^{1}H and ^{13}C paramagnetic shifts of thymidine bound to ϵ186/θ/Dy^{3+}, ϵ186/θ/Tb^{3+}, and ϵ186/θ/Er^{3+}, respectively. Error bars reflect the uncertainty of measurement and are particularly wide for the unresolved ^{1}H NMR signals of H2′ and H2″. The back-calculated $\Delta\delta^{PCS}$ values refer to the best Xplor structure calculated using PCS data from all three metal ions.

the different tumbling properties of free and bound ligand, paramagnetic effects are much larger and have the additional advantage of being scalable over a wide range by the choice of the metal ion. In the case of the strongly paramagnetic lanthanides Dy^{3+}, Tb^{3+}, and Er^{3+} bound to ϵ186/θ, paramagnetic line broadening of thymidine is at least 2 orders of magnitude larger than the line broadening due to slower molecular tumbling of thymidine in the 30 kDa complex. The enhanced relaxation of ligand resonances due to binding to a paramagnetically labeled protein has been shown to enable screening experiments at much reduced protein concentration.[29−31]

Transferred NOE and cross-correlatated relaxation are intramolecular effects and therefore only report on the conformation of the ligand in the bound state. Transferred dipolar couplings,[32,33] which have a great potential for studying complexes of membrane proteins,[34] provide additional information about relative orientation with respect to the protein. Transferred PCS are unique among the transferred NMR effects in that they refer to a unique point (the metal position) and coordinate system (as spanned by the $\Delta\chi$ tensor) which are anchored in the macromolecule and therefore allow the simultaneous determination of the ligand conformation, orientation, and location. In effect, this amounts to the determination of the 3D structure of the complex.

Versatility of Lanthanide Labeling. Due to the symmetry of the $\Delta\chi$ tensor with respect to 180° rotations about its principal axes, a given set of PCS values from a single lanthanide ion can in principle be fulfilled by four symmetry-related locations/orientations of a chiral ligand molecule. In the case of the ϵ186/θ/Ln^{3+}/thymidine complex, only one of the four degenerate solutions avoided severe steric clashes with the protein. More generally, the four-fold degeneracy can be lifted by the use of a second lanthanide ion with a differently oriented $\Delta\chi$ tensor.[35] Due to the chemical similarity among the lanthanide series, any lanthanide ion can bind to a generic lanthanide binding site, allowing the choice between a wide range of $\Delta\chi$ tensors.[36]

For proteins devoid of natural metal binding sites, the prerequisite of a site-specifically attached lanthanide ion can be fulfilled by different lanthanide-binding tags that have recently become available.[37−43] Tags offer additional options to vary the $\Delta\chi$ tensor by the choice of the tag[42] or its attachment at different sites. Due to the long-range nature of the paramagnetic effects, the lanthanide ion does not have to be close to the ligand binding site and can be positioned strategically for binding studies. In the ϵ186/θ/Ln^{3+}/thymidine complex, the close proximity of nucleotide and metal binding sites required very large thymidine concentrations to overcome paramagnetic line broadening.

As PCS depend on the distance between the nuclear spin and the metal ion with r^{-3} as opposed to the r^{-6} dependence of paramagnetic line broadening, PCS values could, in general, be measured with higher precision for systems in which the lanthanide and ligand binding sites are farther apart. A similar improvement would be expected for lanthanides with smaller anisotropy $\Delta\chi$, yet comparable ratio $\Delta\chi_{ax}/\chi$ of anisotropic and isotropic magnetic susceptibilities. Additional broadening of the ligand resonances due to exchange between the bound and free states scales with r^{-6}, $(\Delta\chi_{ax})^2$, and the binding affinity (K_D^{-1}) but is a minor contribution to the line width in the ϵ186/θ/Ln^{3+}/

(24) Balaram, P.; Bothner-By, A. A.; Breslow, E. *Biochemistry* **1973**, *12*, 4695−4704.
(25) Clore, G. M.; Gronenborn, A. M. *J. Magn. Reson.* **1983**, *53*, 423−442.
(26) Ni, F. *Prog. Nucl. Magn. Reson. Spectrosc.* **1994**, *26*, 517−606.
(27) Carlomagno, T.; Felli, I. C.; Czech, M.; Fischer, R.; Sprinzl, M.; Griesinger, C. *J. Am. Chem. Soc.* **1999**, *121*, 1945−1948.
(28) Blommers, M. J. J.; Stark, W.; Jones, C. E.; Head, D.; Owen, C. E.; Jahnke, W. *J. Am. Chem. Soc.* **1999**, *121*, 1949−1953.
(29) Jahnke, W.; Rüdisser, S.; Zurini, M. *J. Am. Chem. Soc.* **2001**, *123*, 3149−3150.
(30) Jahnke, W.; Floersheim, P.; Ostermeier, C.; Zhang, X.; Hemmig, R.; Hurth, K.; Uzunov, D. P. *Angew. Chem., Int. Ed.* **2002**, *41*, 3420−3423.
(31) Bertini, I.; Fragai, M.; Lee, Y.-M.; Luchinat, C.; Terni, B. *Angew. Chem., Int. Ed.* **2004**, *43*, 2254−2256.
(32) Shimizu, H.; Donohue-Rolfe, A.; Homans, S. W. *J. Am. Chem. Soc.* **1999**, *121*, 5815−5816.
(33) Bolon, P. J.; Al Hashimi, H. M.; Prestegard, J. H. *J. Mol. Biol.* **1999**, *293*, 107−115.
(34) Koenig, B. W.; Mitchell, D. C.; König, S.; Grzesiek, S.; Litman, B. J.; Bax, A. *J. Biomol. NMR* **2002**, *16*, 121−125.
(35) Pintacuda, G.; Park, A. Y.; Keniry, M. A.; Dixon, N. E.; Otting, G. *J. Am. Chem. Soc.* **2006**, *128*, 3696−3702.
(36) Bertini, I.; Janik, M. B. L.; Lee, Y.-M.; Luchinat, C.; Rosato, A. *J. Am. Chem. Soc.* **2001**, *123*, 4181−4188.
(37) Wöhnert, J.; Franz, K. J.; Nitz, M.; Imperiali, B.; Schwalbe, H. *J. Am. Chem. Soc.* **2003**, *125*, 13338−13339.
(38) Ikegami, T.; Verdier, L.; Sakhaii, P.; Grimme, S.; Pescatore, B.; Saxena, K.; Fiebig, K. M.; Griesinger, C. *J. Biomol. NMR* **2004**, *29*, 339−349.
(39) Pintacuda, G.; Moshref, A.; Leonchiks, A.; Sharipo, A.; Otting, G. *J. Biomol. NMR* **2004**, *29*, 351−361.
(40) Prudencio, M.; Rohovec, J.; Peters, J. A.; Tocheva, E.; Boulanger, M. J.; Murphy, M. E. P.; Hupkes, H.-J.; Kosters, W.; Impagliazzo, A.; Ubbink, M. *Chem. Eur. J.* **2004**, *10*, 3252−3260.
(41) Leonov, A.; Voigt, B.; Rodriguez-Castañeda, F.; Sakhaii, P.; Griesinger, C. *Chem. Eur. J.* **2005**, *11*, 3342−3348.
(42) Haberz, P.; Rodriguez-Castañeda, F.; Junker, J.; Becker, S.; Leonov, A.; Griesinger, C. *Org. Lett.* **2006**, *8*, 1275−1278.
(43) Su, X. C.; Huber, T.; Dixon, N. E.; Otting, G. *ChemBioChem.* **2006**. In press.

thymidine complex (see Supporting Information). Tighter binding ligands could thus be studied with lanthanide ions located at larger distances or with smaller magnetic susceptibility tensors.

Implications for Structure-Based Drug Design. The method described here opens exciting opportunities for rational drug design, as it yields 3D structures of complexes between proteins and small chemical compounds in solution with unprecedented ease and accuracy. No isotope labeling of the ligand molecule is required, although isotope enrichment can be used to overcome the low sensitivity of ^{13}C NMR experiments for compounds of limited solubility. The $\Delta\chi$ tensor of the lanthanide ions can readily be determined from ^{15}N-labeled samples of the protein by comparison with the crystal or solution structure.[2,3] Once the magnitude of the $\Delta\chi$ tensor and its location and orientation with respect to the protein have been determined, all subsequent experiments can be performed using protein at natural isotopic abundance.

In contrast to many other NMR parameters, the measurement of transferred paramagnetic shifts is straightforward and only requires simple 1D NMR spectra. Further, the possibility of detecting ^{13}C spins makes the method particularly powerful for many pharmacologically relevant compounds which have too few protons for determination of the complex structure from intermolecular NOEs. We anticipate that transferred PCS will be applicable to a wide range of targets of pharmaceutical importance.

Acknowledgment. M.J. thanks the Humboldt Foundation for a fellowship. G.P. acknowledges support by the CNRS and the French research ministry (Grant ANR Jeunes Chercheurs 2005). Financial support from the Australian Research Council for a Federation Fellowship for G.O. and the 800 MHz NMR spectrometer at ANU is gratefully acknowledged.

Supporting Information Available: Derivation of eq 3, an estimate of exchange broadening, binding affinities of TMP and thymidine to $\epsilon 186/\theta$, measured paramagnetic shifts of thymidine, ^{1}H NMR spectra of thymidine in the presence of $\epsilon 186/\theta/Ln^{3+}$, correlation of measured and back-calculated paramagnetic shifts of thymidine for the structures calculated from single lanthanide ions, stereoviews of the seven best ϵ186/thymidine structures calculated from data with different lanthanide ions. This material is available free of charge via the Internet at http://pubs.acs.org.

JA063584Z